Mode instability in high power fiber amplifiers

Arlee V. Smith[*] and Jesse J. Smith
AS-Photonics, LLC, 8500 Menaul Blvd. NE, Suite B335, Albuquerque, NM 87112, USA
[*]*arlee.smith@as-photonics.com*

Abstract: For powers exceeding a sharp threshold in the vicinity of several hundred watts the beam quality from some narrow bandwidth fiber amplifiers is severely degraded. We show that this can be caused by transverse thermal gradients induced by the amplification process.

OCIS codes: (060.2320) Fiber optics amplifiers and oscillators; (060.4370) Nonlinear optics, fibers.

References and links

1. C. Jauregui, T. Eidam, J. Limpert, and A. Tünnermann, "The impact of modal interference on the beam quality of high-power fiber amplifiers," Opt. Express **19,** 3258–3271 (2011), http://www.opticsinfobase.org/abstract.cfm?URI=oe-19-4-3258.
2. T. Eidam, S. Hanf, E. Seise, T. V. Andersen, T. Gabler, C. Wirth, T. Schreiber, J. Limpert, and A. Tünnermann, "Femtosecond fiber CPA system emitting 830 W average output power," Opt. Lett. **35,** 94–96 (2010), http://www.opticsinfobase.org/abstract.cfm?URI=ol-35-2-94.
3. F. Stutzki, F. Jansen, T. Eidam, A. Steinmetz, C. Jauregui, J. Limpert, and A. Tünnermann, "High average power large-pitch fiber amplifier with robust single-mode operation," Opt. Lett. **36,** 689–691 (2011), http://www.opticsinfobase.org/abstract.cfm?URI=ol-36-5-689.
4. J. W. Arkwright, P. Elango, G. R. Atkins, T. Whitbread, and M. J. F. Digonnet, "Experimental and theoretical analysis of the resonant nonlinearity in ytterbium-doped fiber," J. Lightwave Tech. **16,** 798–806 (1998), http://www.opticsinfobase.org/abstract.cfm?URI=jlt-16-5-798.
5. A. A. Fotiadi, O. L. Antipov, and P. Mégret, "Resonantly induced refractive index changes in Yb-doped fibers: the origin, properties and application for all-fiber coherent beam combining," in *Frontiers in Guided Wave Optics and Optoelectronics*, B. Pal, ed. (Intec, 2010), pp. 209–234.
6. N. Andermahr and C. Fallnich, "Optically induced long-period fiber gratings for guided mode conversion in few-mode fiber," Opt. Express **18,** 4411–4416 (2010), http://www.opticsinfobase.org/abstract.cfm?URI=oe-18-5-4411.
7. M. Chi, J.-P. Huignard, and P. M. Petersen, "A general theory of two-wave mixing in nonlinear media," J. Opt. Soc. Am. B **26,** 1578–1584 (2009), http://www.opticsinfobase.org/abstract.cfm?URI=josab-26-8-1578.
8. R. Soulard, A. Brignon, J.-P. Huignard, and R. Moncorgé, "Non-degenerate near-resonant two-wave mixing in diode pumped Nd^{3+} and Yb^{3+} doped crystals in the presence of athermal refractive index grating," J. Opt. Soc. Am. B **27,** 2203–2210 (2010), http://www.opticsinfobase.org/abstract.cfm?URI=josab-27-11-2203.
9. M. D. Feit and J. A. Fleck, Jr. "Light propagation in graded-index optical fibers," Appl. Opt. **17,** 3990–3998 (1978).
10. L. L. Zhang, P. Shi, and L. Li, "Semianalytical thermal analysis of rectangle Nd:GGG in heat capacity laser," Appl. Phys. B **101,** 137–142 (2010).

1. Introduction

Published [1–3] and anecdotal reports indicate that high power, cladding pumped Yb^{3+} doped fiber amplifiers often exhibit a sharp power threshold above which severe modal degradation occurs. The threshold varies with fiber design and operating conditions, usually falling in the range of 100-1500 W. Further, the output beam profile may exhibit temporal instability, ranging from quasi periodic fluctuations in the 1-5 kHz range to quite chaotic behavior. This modal degradation sets the practical upper power limit for these amplifiers, so it is important to understand its cause with the hope of finding ways to prevent it.

Jauregui *et al.* [1] suggested the cause is refractive index changes in the core induced by variations in the population of the upper lasing level of the Yb^{3+} ions. The invoked refractive index change due to population inversion, which we will refer to as the Kramers-Kronig (KK) effect, is well known, and it has been measured for Yb-doped silica fiber [4, 5]. Using a beam propagation model that included steady-state computations of the upper state population and refractive index modification at each point in the fiber, Jauregui *et al.* demonstrated that this effect is strong enough to cause a substantial power transfer from the fundamental transverse mode to higher order modes. They also suggested the alternative mechanism of nonuniform heating of the core acting through the thermo optic effect to create similar variations in the refractive index near the core.

In this paper we also use a beam propagation model to study mode coupling via the same two effects, KK and thermal, but rather than assuming steady-state behavior, we allow for transient evolution of the populations and temperature profiles. This added dimension will prove crucial in realizing exponential gain of the power in high order modes, with the consequence of sharp power thresholds for modal degradation.

As is well known, the transverse modes of optical fiber are quite robust. Light in a single mode tends to stay in that mode unless the refractive index profile changes significantly over a distance less than several intermodal beat lengths. Random variations in the refractive index profile can incoherently couple light from the fundamental mode to higher order modes. Random micro bends on a short length scale can do the same. However, if the index profile varies in a periodic fashion with a period equal to the beat length between two modes, light can be coherently transferred between the two modes. If the refractive index modification is linked to the local irradiance of the guided light, the periodic interference between two modes will cause a periodic index modification with exactly the period required for coherent transfer. Furthermore, if the index change is proportional to the power in a weak mode, that mode can experience exponential gain at the expense of the strong mode.

To qualitatively illustrate mode coupling by refractive index changes in a guiding core, we show in Fig. 1 light in the fundamental LP_{01} mode launched from the left, encountering a wedge of higher refractive index indicated by the triangle. After passing through the wedge the beam has a phase tilt which causes it to initially veer downward and then oscillate up and down. Described in terms of fiber modes, the wedge transfers a small fraction of the light from the fundamental mode to the LP_{11} mode. The fundamental mode, which we will refer to as mode one, has a near-Gaussian profile. The LP_{11} mode, which we will call mode two, has two lobes, upper and lower, with electric fields of opposite sign. Because the fundamental mode cannot fully describe an asymmetric irradiance profile, a shift in the irradiance profile from the core center indicates the presence of mode two. Larger deflection angles and larger oscillation amplitudes correspond to a higher fraction of the light in mode two.

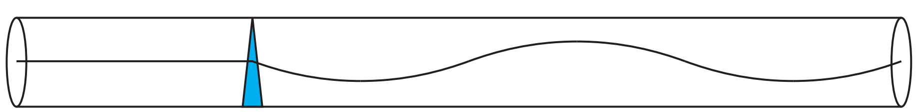

Fig. 1. Light in mode one, traveling to the right encounters a wedge of higher refractive index. The wedge induces a phase tilt which causes the light to oscillate up and down with a period determined by the difference in propagation constants for modes one and two.

The oscillation period is set by the difference in propagation constants of the modes one and two according to $L_{12} = 2\pi/|\beta_1 - \beta_2|$. A set of index wedges positioned every half beat length,

#144718 - $15.00 USD Received 24 Mar 2011; accepted 29 Apr 2011; published 9 May 2011

as shown in Fig. 2, would coherently transfer light from mode one to mode two, leading to a steady growth in the oscillation amplitude and mode two content. In the time reversed picture the light propagates right to left, and a mixture of mode one and two, with the proper initial phases and amplitudes, emerges entirely in mode one.

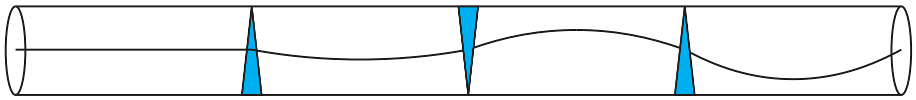

Fig. 2. A properly spaced array of index wedges coherently transfers light from mode one to mode two, leading to large amplitude oscillations, or equivalently to large power transfer from mode one to mode two.

In applying this picture to the KK and thermal effects, we make the usual assumption that the pump light is uniformly distributed across the fiber core. The amplification of the signal light causes the upper state population to be depleted more in regions of high signal irradiance. This reduced upper state population reduces the local refractive index by a small amount due to the KK effect. To a first approximation the result is a refractive index wedge located at each maximum excursion point of the oscillating irradiance, and with its apex pointed in the same direction as the irradiance deviation. The reduced upper state population also causes an increase in the local heat deposition rate due to the amplification process, and the resulting local temperature rise leads to an increased refractive index via the thermo optic effect. The thermal wedges are similar to the KK wedges but point in the opposite directions (for Yb^{3+} ions in silica). The thermal wedges are diagrammed in Fig. 3. Of course, the diagrammed wedges are simplified representations of the true light-induced index profiles that have (x,y,z) spatial structure, but the important point is that the actual index-irradiance patterns have the same left-right symmetry as the diagram.

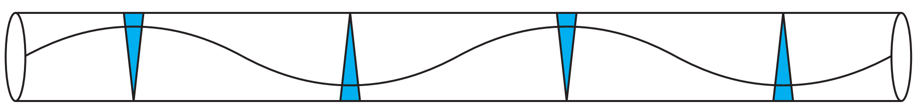

Fig. 3. The sinusoid represents the oscillation in the irradiance profile, the wedges show the symmetry of the thermally-induced refractive index changes.

As we pointed out above, the light-induced index perturbations automatically have the correct period to produce coherent transfer from mode one to mode two. However, there is a second important requirement for strong coupling: a phase shift between the irradiance oscillations and the index tilts. In Fig. 3 a coherent coupling of light from mode one to mode two as the light propagates from left to right would be indicated by an increasing amplitude of the sinusoid in the direction of propagation. Time reversing this process would correspond to light propagating right to left with a decreasing sinusoid amplitude in the direction of propagation. However, the diagram is mirror symmetric left to right, so the mode coupling strength must be zero. Using a beam propagation model that included laser gain plus light induced refractive index changes due to either the KK or the thermal effect, we verified this absence of mode coupling if a steady state population distribution or temperature profile is assumed. However, a phase shift between the index perturbation and the irradiance profile would break the left-right symmetry and allow mode coupling. Such a phase shift is evident in the results in Ref. [6] which illustrates in experiment and model a mode coupling produced by a static index grating written by a counter propagating laser via the Kerr effect.

A phase shift in a self induced index grating can be produced by an irradiance pattern that

#144718 - $15.00 USD Received 24 Mar 2011; accepted 29 Apr 2011; published 9 May 2011

moves along the length of the fiber. This can be achieved by including a frequency shift between the light in modes one and two. The velocity of the grating for a small frequency shift is well approximated by

$$v_{grating} = \frac{c}{\omega} \frac{\omega_2 - \omega_1}{\bar{n}_2 - \bar{n}_1} \tag{1}$$

where ω_1 (ω_2) is the frequency of light in mode one (two), and $\bar{n}_1$ ($\bar{n}_2$) is the effective refractive index of light in mode one (two), determined from the propagation constants of the modes. Because ($\bar{n}_1 > \bar{n}_2$), the choice ($\omega_2 < \omega_1$) causes the irradiance pattern to move in the positive z direction, or downstream, while $(\omega_2 > \omega_1)$ causes it to move upstream. The time lag between the moving irradiance profile and the refractive index changes it causes produces the requisite phase lag. In KK mode coupling the time delay is related to the finite upper state lifetime of the Yb ions. In thermal mode coupling the delay is related to the time of thermal diffusion across the core.

A time delayed index profile is qualitatively diagrammed in Fig. 4 for thermal mode coupling. It is clear that in this case the wedges can cause an increase in the oscillation amplitude as the light propagates from left to right, much like the example in Fig. 2. Further, the Doppler shift from the moving grating means the light transferred from mode one to mode two is red shifted to match the frequency of mode two. Because the sign of the index wedges are reversed for the KK effect, the choice $(\omega_2 > \omega_1)$ causes the irradiance grating to move upstream, and this also produces the proper phase and frequency shifts for power transfer from mode one to mode two. If we chose instead the opposite signs for the frequency offset in either the KK or thermal case, the power transfer would reverse direction, resulting in power transfer from mode two to mode one.

These ideas of moving gratings are similar to those used to describe two beam coupling via transverse refractive index gratings in bulk pumped lasing media [7,8]. Frequency offsets in that case lead to lateral grating motion and lateral phase shifts that cause power transfer between crossed beams.

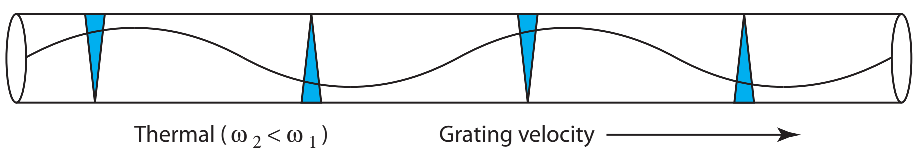

Fig. 4. Like Fig. 3 except there is a frequency offset of the light in modes one and two. Because $(\omega_2 < \omega_1)$ the irradiance grating moves downstream, and the time lag of the induced temperature profile caused by thermal diffusion makes the refractive index pattern lag the irradiance profile.

In the following sections we first present the parameters of the fiber amplifier we have chosen to illustrate mode coupling. We then describe in detail separate computations of mode coupling due to the KK effect and due to the thermal effect.

2. Parameters of the modeled fiber

To exercise our mode coupling models we use a step index fiber with the parameters listed in Table 1. Although these parameters are typical of those found in high power Yb doped amplifiers, they do not represent any actual fiber amplifier. The pump and mode one signal powers as a function of distance along the fiber, computed in the absence of mode coupling, are shown in Fig. 5.

#144718 - $15.00 USD Received 24 Mar 2011; accepted 29 Apr 2011; published 9 May 2011

Table 1. Parameters of Test Amplifier

d_{core}	30 μm	d_{dopant}	30 μm
d_{clad}	250 μm	N_{Yb}	3.25×10^{25} m^{-3}
λ_p	976 nm	λ_s	1064 nm
σ_p^a	2.47×10^{-24} m^2	σ_p^e	2.44×10^{-24} m^2
σ_s^a	5.80×10^{-27} m^2	σ_s^e	2.71×10^{-25} m^2
P_p	1200 W	P_s	30 W
dn/dT	1.2×10^{-5}	L	5 m
n_{core}	1.452	n_{clad}	1.45
τ	901 μs	Δ_{KK}	1.2×10^{-30} m^3
R_{bend}	∞		

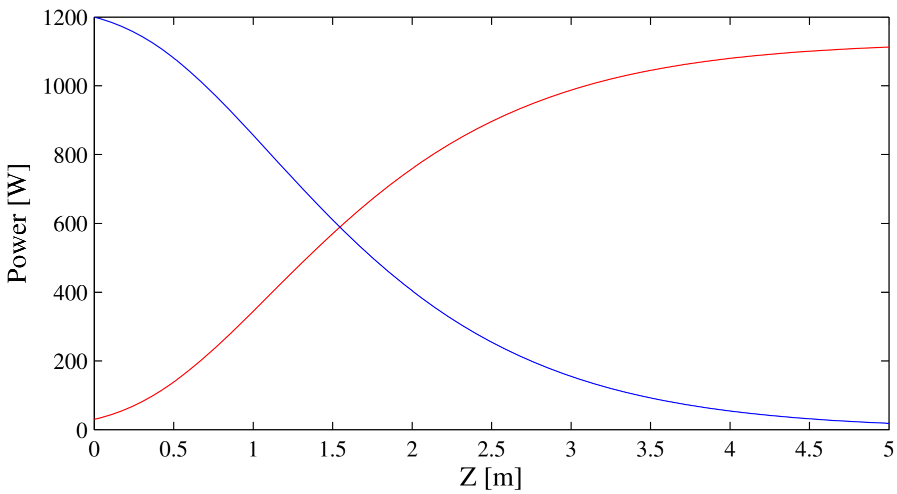

Fig. 5. Pump and signal powers versus z for the modeled fiber amplifier in the absence of mode coupling. The input powers are [1200, 30, 0] W for [pump, mode one, mode two].

3. KK mode coupling

3.1. Time response of a driven damped system

We stated above that the time delay in the KK model is related to the upper state lifetime of the Yb ions. We can make the discussion of phase lags and mode coupling more quantitative by considering the response of a driven damped system that represents the time response of the upper state population at a single spatial point in the fiber core. The driving term is assumed to have a single frequency component at ω and a damping time of τ. The equation for the point response U is

$$\frac{dU}{dt} = R - \frac{U}{\tau} \tag{2}$$

and we assume a driving term of the form

$$R = R_\circ[1 + \alpha \sin(\omega t)]. \tag{3}$$

The solution is

$$U = R_\circ \tau \left[1 + \frac{\alpha}{\sqrt{1+\omega^2\tau^2}} \sin(\omega t - \delta)\right], \tag{4}$$

Received 24 Mar 2011; accepted 29 Apr 2011; published 9 May 2011
23 May 2011 / Vol. 19, No. 11 / OPTICS EXPRESS 10184

where the phase lag δ satisfies

$$\sin\delta = \frac{\omega\tau}{\sqrt{1+\omega^2\tau^2}}. \tag{5}$$

If we make the reasonable conjecture that the coupling strength S is proportional to $U\sin(\delta)$, we have

$$S \propto \frac{\omega\tau}{1+\omega^2\tau^2}, \tag{6}$$

so the strongest coupling occurs at a driving frequency of $\omega = 1/\tau$, where $\delta = 45^\circ$. Of course this single point calculation is a rather crude approximation for the actual mode coupling strength, but it should predict the frequency offset associated with the strongest mode coupling to within a factor of two.

3.2. Transient KK mode coupling

In our detailed KK numerical mode coupling model we use the time dependent equation for the upper state population fraction,

$$\frac{dn_u}{dt} = (P_p\sigma_p^a/Ah\nu_p + I_s\sigma_s^a/h\nu_s)n_l - (P_p\sigma_p^e/Ah\nu_p + I_s\sigma_s^e/h\nu_s + 1/\tau)n_u, \tag{7}$$

to compute the phase retarded upper state population distribution throughout the core. Here, P_p is the pump power, A is the pump cladding area, and we make the usual assumption that the pump light is uniform across the full cross section of the pump cladding. The σs are absorption and emission cross sections. I_s is the signal irradiance that varies with (x,y,t) due to modal interference. Note that we can define an effective upper state population lifetime τ_{eff}, accounting for the pump and signal stimulating emission from the upper level,

$$1/\tau_{\text{eff}} = P_p\sigma_p^e/Ah\nu_p + I_s\sigma_s^e/h\nu_s + 1/\tau. \tag{8}$$

At the input end of our test amplifier $\tau_{\text{eff}} \approx 2\ \mu$s near the mode center. The heuristic model presented in Sec. 3.1 suggests, according to Eq. (6), that the highest mode coupling gain at the input should occur at a frequency offset of approximately 80 kHz. The same analysis suggests the peak mode coupling gain near the output should lie near 350 kHz.

The refractive index changes that induce mode coupling are computed using

$$\Delta n\ =\ N_{Yb}\, n_u\, \Delta_{KK} \tag{9}$$

where N_{Yb} is the Yb^{3+} density, and Δ_{KK} is the KK coefficient at 1064 nm. The value for Δ_{KK} listed in Table 1 is consistent with the value used by Jauregui *et al.* [1], but it is approximately ten times the value of Arkwright *et al.* [4], based on our analysis of the experimental data presented in Ref. [4].

4. Transient thermal mode coupling

We can make a similar estimate of the frequency offset required for maximal thermal mode coupling. The time lag of the temperature profile relative to the heat deposition profile is due to thermal diffusion. For silica the thermal diffusion time can be found using $\rho = 2201$ kg/m^3, $C = 703$ J/m^{2}K, and $K = 1.38$ W/K-m in the expression for the thermal diffusion time

$$\tau = \frac{C\rho}{K}r^2 = 1.12\times 10^6\ r^2. \tag{10}$$

The thermal diffusion time for $r \approx 10\ \mu$m is approximately 100 μs which is long compared with the effective upper state lifetime in a strongly driven fiber (see Section 3). This allows us

#144718 - $15.00 USD Received 24 Mar 2011; accepted 29 Apr 2011; published 9 May 2011

to use the steady state approximations for the upper state population and the heat deposition profile at each time point in the modal beat cycle. The steady state expression for the upper state population fraction is

$$n_u = \frac{P_p \sigma_p^a / h\nu_p A + I_s \sigma_s^a / h\nu_s}{P_p(\sigma_p^a + \sigma_p^e)/h\nu_p A + I_s(\sigma_s^a + \sigma_s^e)/h\nu_s + 1/\tau}. \tag{11}$$

Based on this population profile, we compute the heat deposition rate Q from the pump absorption and the quantum defect using

$$Q = N_{Yb}\left[\frac{\nu_p - \nu_s}{\nu_p}\right]\left[\sigma_p^a - (\sigma_p^a + \sigma_p^e)n_u\right]\frac{P_p}{A}, \tag{12}$$

where the first term in brackets is the quantum defect. We insert this Q profile in the thermal diffusion equation

$$\rho C \frac{dT}{dt} = Q + K\left(\frac{\partial^2 T}{\partial x^2} + \frac{\partial^2 T}{\partial y^2}\right) \tag{13}$$

and integrate in time to find $T(x,y,t)$. We assume the longitudinal heat flow is negligible. After the temperature profile is found we compute the refractive index change using the thermo optic coefficient for silica,

$$\Delta n = 1.2 \times 10^{-5} \Delta T. \tag{14}$$

5. The beam propagation models

Our beam propagation model, which includes the phase lagged refractive index profile, is straightforward, but it is computationally intensive and slow. We initiate the model by constructing an optical field containing most of the light in mode one at frequency one, with a small fraction in mode two at frequency two. Exactly one complete time cycle ($0 \leq t < |1/\Delta\nu|$) of this signal field is discretized on an (x,y,t) grid. For the KK model Eq. (7) is integrated in time to find $n_u(x,y,t)$. The driving term is assumed to be periodic in time, allowing the time integration to be carried forward through multiple cycles until the transients become inconsequential. One full cycle of the resulting periodic upper state population distribution is used in Eq. (9) to find the full cycle of refractive index modifications. Each of the time slices of the optical field over a complete cycle are propagated independently using the corresponding full cycle modified index profile. In other words, for each z step we model one complete cycle of the moving irradiance and its associated lagging index gratings as they pass through the current z location. The depleted pump power is also computed for the full time cycle, and used in subsequent propagation steps. However, in the results presented here we find that the time modulation of the pump is negligibly small. Diffractive beam propagation is modeled using a split step method in which the laser gain and refractive-index-induced phase for one z-step are added to the optical field in the first half of the propagation step, and the beam is propagated in the second half step using FFT methods [9]. This modeling technique correctly incorporates the phase shift between the irradiance and refractive index profiles, and induces the Doppler shifts necessary for power transfer between modes.

The thermal beam propagation model is similar except the steady state value of n_u is computed from Eq. (11) and used as the drive term in Eq. (13). We used a 64×64 grid in the x,y dimension, with a total grid size of 75×75 μm. For convenience the thermal diffusion equation is solved in k-space by performing xy sine transforms on T and Q, then numerically integrating the transformed diffusion equation to find their time dependent values. A second set of xy sine transforms yields $T(x,y,t)$. Our method is similar to that used by Zhang *et al.* [10]. The use of sine expansions means the temperature change is clamped at zero on the square boundary of

Received 24 Mar 2011; accepted 29 Apr 2011; published 9 May 2011
23 May 2011 / Vol. 19, No. 11 / OPTICS EXPRESS 10186

the computation grid, but by making the physical size of the grid large compared with the light confining core, the errors in the computed temperature gradients near the core are acceptable. The overall temperature near the core is not important for mode coupling. Other methods of computing $T(x,y,t)$ could be used to accommodate more general boundary conditions such as a fixed temperature on a circular boundary. As in the KK model, multiple cycles of the field are stitched together so the time integration can be extended until the transients become negligible. Figure 6 shows computed irradiance and temperature profiles at the input end of the amplifier with the usual pump and mode one powers of 1200 W and 30 W, plus 10 W in mode two. We use this large mode two content to make the oscillations and phase lag more apparent in the linked movie (Media 1).

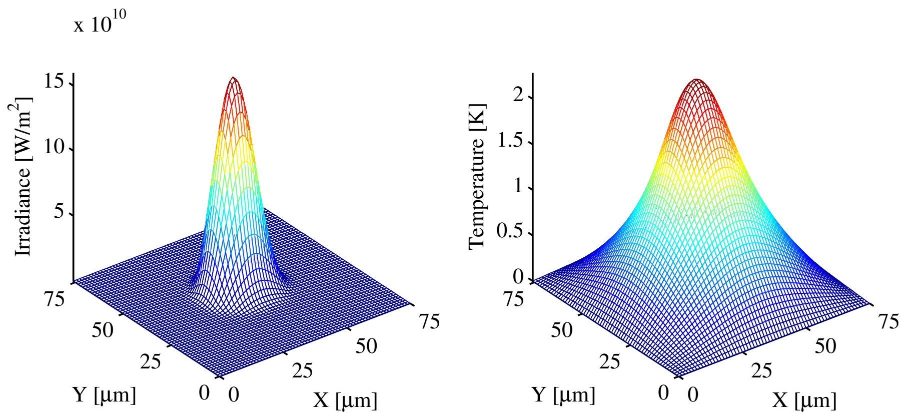

Fig. 6. Irradiance profile (left) and temperature profile (right) at the input end of the amplifier. The powers are 1200 W pump, 30 W mode one, 10 W mode two, and the frequency offset between modes is 2 kHz. In this illustration we use an exagerated mode two power to dramatize the oscillations of the irradiance and temperature profiles. The phase delay of the temperature relative to the irradiance is readily apparent in the movie (Media 1).

After a number of propagation steps are completed, the field is decomposed into modes one and two to determine their complex amplitudes over one complete beat cycle. These time sequenced amplitudes are then Fourier transformed to find the frequency spectrum of each mode. As anticipated, we find that in both the thermal and the KK models, light is transferred from mode one to mode two if the sign of the frequency offset matches the discussion above. If the frequency offset is reversed, the direction of power transfer is also reversed. Because we are interested in power transfer from mode one to mode two, we make the frequency offset of mode two negative for the thermal effect ($\omega_2 < \omega_1$) and positive for the KK effect.

6. KK mode coupling model results

We applied this model to the test amplifier of Table 1 to compute the small signal gain of mode two as a function of the offset frequency at several positions along the fiber. We propagate a few mm for each z location and each frequency and then use

$$\frac{dP_{s2}}{dz} = g(z,\Delta\nu)P_{s2} \tag{15}$$

to compute g based on the increase in mode two power. These gain values at various z locations are plotted in Fig. 7 as a function of the frequency offset $\Delta\nu$. The values of P_{s1} and P_p at each z

#144718 - $15.00 USD
Received 24 Mar 2011; accepted 29 Apr 2011; published 9 May 2011

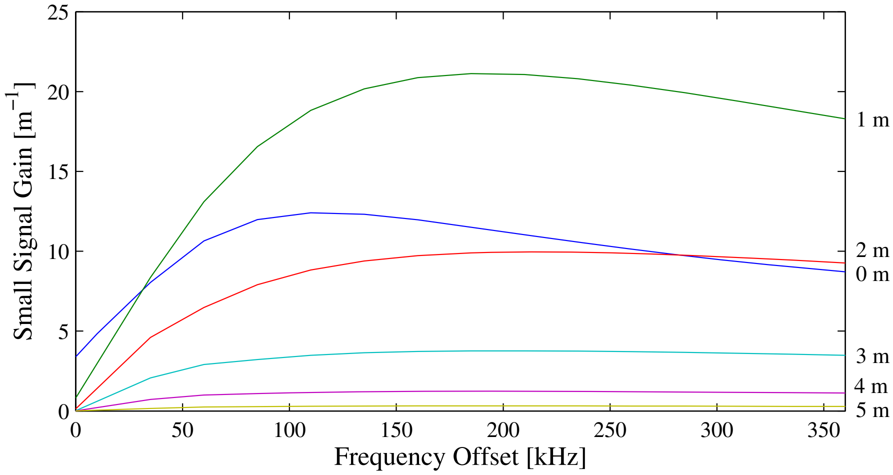

Fig. 7. Small signal gain of mode two versus frequency offset ($\nu_2 - \nu_1$) for different z positions along the fiber. The laser gains are included and can be found from the left axis intercepts.

location are taken from the curves of Fig. 5. The shapes of the curves of gain versus frequency at z=0 and z=1 m are well fit by functions with the form of Eq. (6), and with the peak at approximately the predicted frequencies based on the effective lifetimes.

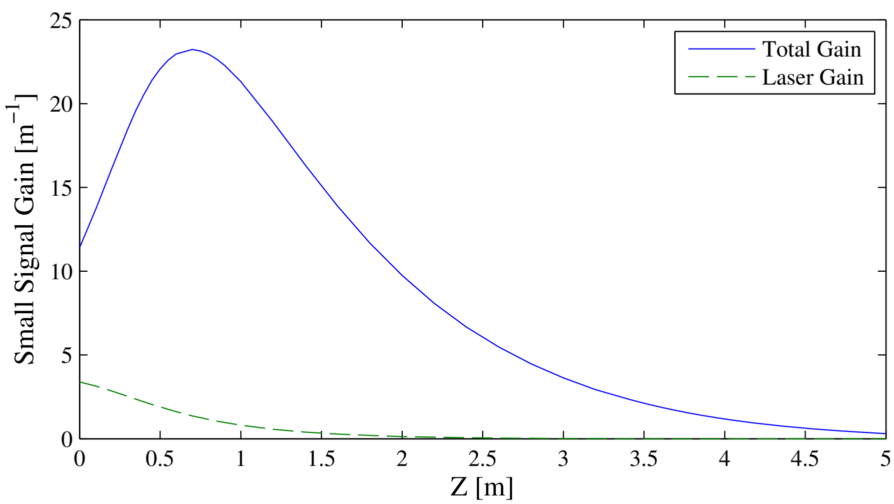

Fig. 8. Small signal gain of mode two at 200 kHz for the test amplifier. The solid curve is total gain of mode two; the dashed curve shows the contribution of laser gain.

Assuming the power in mode 2 remains small, we can express it as

$$P_{s2}(z) = P_{s2}(0)e^{G(z)} \tag{16}$$

where $G(z)$ is the integral of the small signal gain,

$$G(z) = \int_0^z g(z')dz'. \tag{17}$$

Summing the gain curves of Fig. 7 gives an approximation of $G(L)$ that indicates the frequency offset that maximizes $G(L)$ lies near 200 kHz. We computed the small signal gain $g(z)$ at 200 kHz for a fine set of z intervals and display the result in Fig. 8. Finally, we ran the KK model over an extended length of fiber with the usual launched powers of 1200 W in the pump and 30 W in mode one, plus 1 μW in mode two. The model results are shown in Fig. 9.

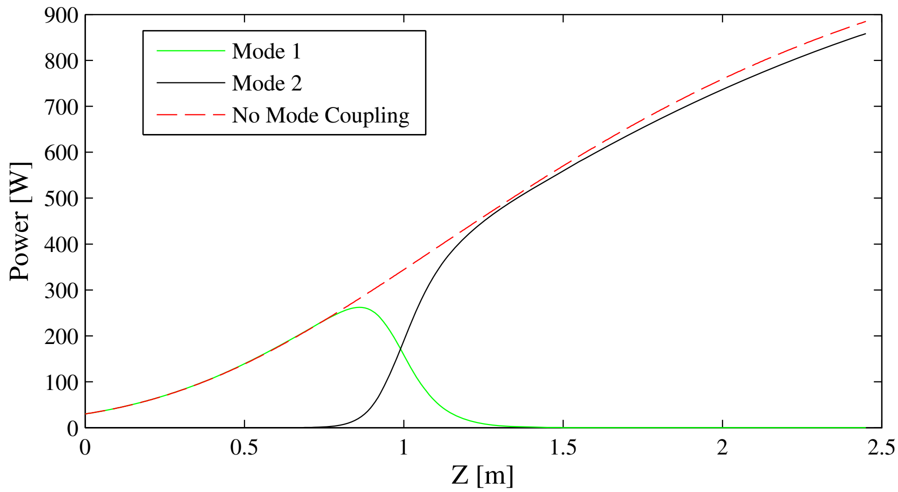

Fig. 9. KK coupling at 200 kHz with inputs of [1200, 30, 1E-6] W for [pump, mode one, mode two]. The dashed curve shows mode one power without mode coupling.

Initially mode two is weak, and mode one is amplified just as though there were no mode coupling, but after approximately one meter the power is abruptly transferred from mode one to mode two where it remains thereafter. The amplification of mode two is slightly less than that of mode one beyond one meter because of poorer overlap of mode two with the doped core, so the power in mode two falls slightly below the reference curve for mode one. The light that is transferred from mode one to mode two is also frequency shifted to match the frequency of mode two. As a caution we note that the value of the KK coupling coefficient is quite uncertain, and the value we have used may be too large by an order of magnitude or more. However, this model serves to illustrate mode coupling, and the chosen coupling coefficient leads to a mode coupling strength similar to the thermal coupling described next.

7. Thermal mode coupling model results

The thermal coupling coefficient is much better known than the KK coefficient so we are confident that the thermally induced gains presented here are quite accurate. Figure 10 shows the small signal gain of mode two versus the frequency difference $(\nu_1 - \nu_2)$ at several positions along the test amplifier. Near the input the gain peaks near 2.5 kHz, and the peak shifts to approximately 2 kHz at one meter and later. Unlike the corresponding curves for KK coupling (Fig. 7), the curves near the input end are not well fit by the form in Eq. (6). This is not surprising because the phase delay in this case is not local as in KK, but is due to thermal diffusion.

The thermal model runs much slower than the KK model because integrating the thermal diffusion equation requires fine time steps for convergence. The maximum time step is fixed by the x,y dimensions and the diffusion constant, so the computation time and the required memory increase with a decreasing frequency offset, making the computation especially slow for frequency offsets less than a few kHz. For this reason we have not attempted to propagate over

#144718 - $15.00 USD
Received 24 Mar 2011; accepted 29 Apr 2011; published 9 May 2011

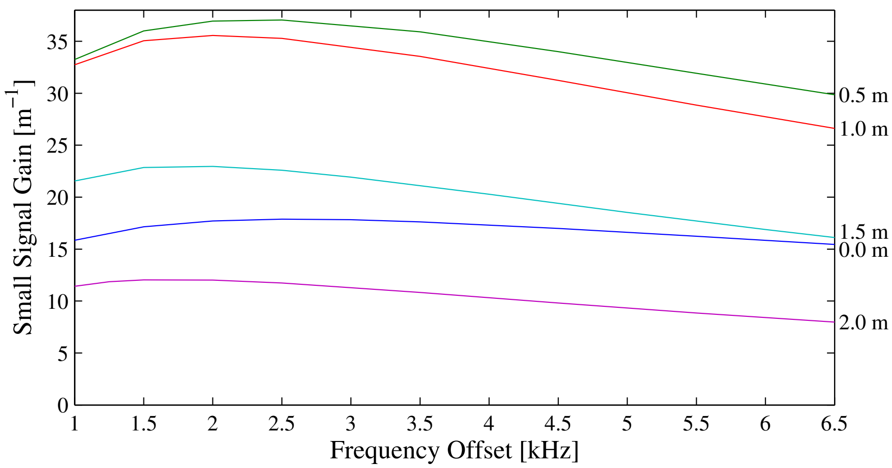

Fig. 10. Small signal gain of mode two versus frequency offset ($\nu_1 - \nu_2$) for different z positions along the fiber. The laser gain is included but it is a small fraction of the small signal gain.

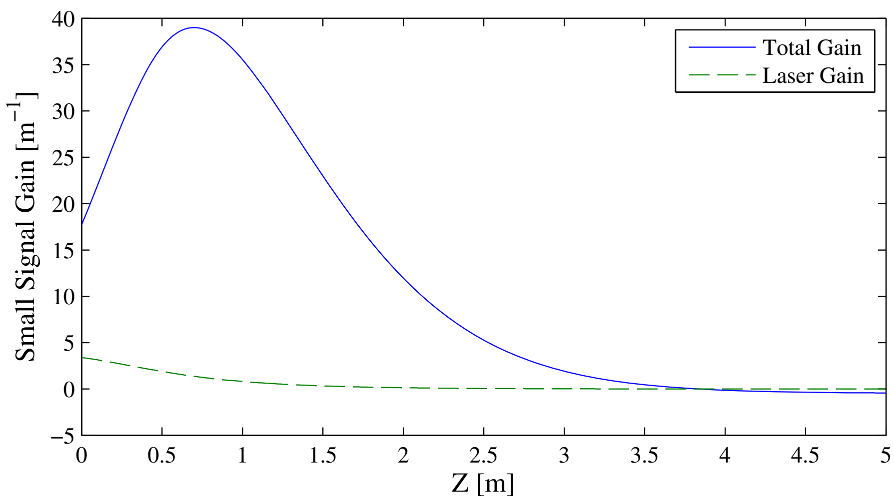

Fig. 11. Small signal gain of mode two at 2 kHz versus z for the test amplifier. The solid curve is total gain of mode two and the dashed line is the contribution of laser gain. The mode coupling gain is the difference between the two curves.

a long fiber section as we demonstrated using the KK model, but we can compute the small signal gains by propagating over short distances. We propagate a distance of one beat length L_{12} or half that, because at these distances all times in the full time cycle experience identical gains. A similar procedure with the KK model gave good agreement between the net gain calculated by integrating the small signal gains computed from short propagation lengths, and the net gain computed directly by propagating over the full distance. Figure 11 shows the small signal gain of mode two due to thermal coupling at a frequency offset of 2 kHz. This frequency offset was chosen to maximize the net gain along the fiber, based on the curves in Fig. 10. The slightly negative gain near the output end an artifact of the short propagation distances used in computing the gain.

We modeled the test amplifier with pump powers of 600 W and 900 W in addition to 1200 W, and plot the integrated gain coefficients $G(L)$ as symbols in Fig. 12. The value of $G(L)$ is nearly linear in the pump power, so the total gain of mode two grows exponentially with the pump power. This will result in a sharp threshold in pump power for mode degradation via thermally induced transfer of light from mode one to mode two.

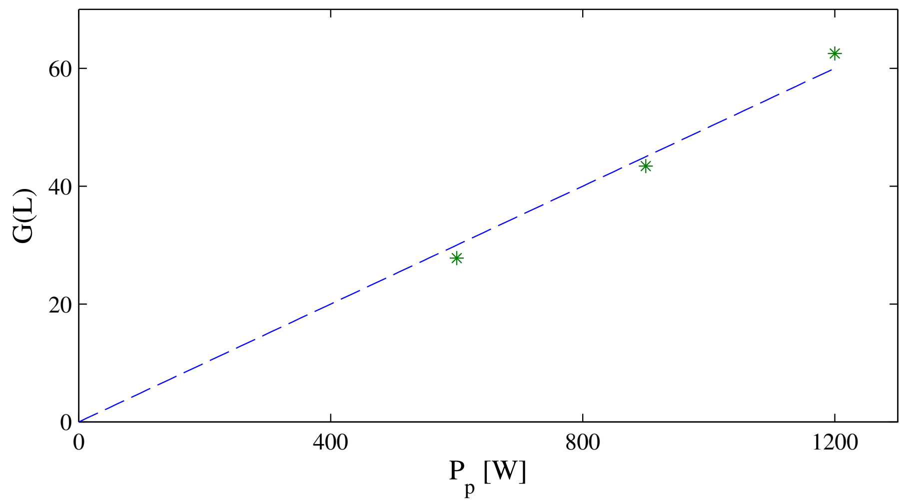

Fig. 12. Net gain of thermal mode coupling versus pump power. The symbols are the integrated small signal gains of mode two for three pump powers. The dashed line is for comparison with a linear dependence on pump power.

Comparison of the KK and thermal gain curves in Figs. 9 and 11 reveals that thermal mode coupling is much stronger than KK mode coupling near the amplifier input end, but falls more rapidly near the output end. The integrated small signal gain for KK coupling at 200 kHz is $G(L) = 44.3$; that for thermal coupling at 2 kHz is $G(L) = 62.5$, so thermal mode coupling is stronger than KK coupling even for a KK coefficient that is perhaps too large.

8. Conclusions

Our model makes several simplifying assumptions. For example, we assumed only modes one and two are populated, and the light in each is monochromatic with a fixed frequency separation. Nevertheless, we think our results strongly indicate that thermal, and perhaps KK, mode coupling can cause mode degradation in laboratory amplifiers. In reality other modes will also be coupled to modes one and two. This can introduce mode coupling losses to mode two that will partially counteract the gain we have computed. This power flow to additional modes may add to the mode degradation, and given the extremely high gains we have computed, the power flow to a variety of modes could be substantial.

Our assumption of monochromatic light is not limiting either. Our results should apply to broadband light in modes one and two if they have frequency components with the right frequency offsets for high gain. The gain bandwidth for mode coupling is quite broad relative to the frequency at maximum gain, so components within a broad range can be amplified. The expected result is fluctuating mode coupling and mode degradation. A Fourier transform of the fluctuations would provide the spectrum of amplification.

Our assumed initial condition of almost all of the light is in mode one with a small amount

#144718 - $15.00 USD
Received 24 Mar 2011; accepted 29 Apr 2011; published 9 May 2011

seeding mode two raises the question of the source of the mode two seed light. Its origin is not entirely clear. The weak seed could be created by mechanical vibration of the fiber, particularly at the fiber input where coupling into the fiber is highly position sensitive, or it could be created by oscillations in the pump power or spectra, or by fluorescence from the upper laser level, or it might be present in the injected signal light.

Detailed experimental studies will be necessary to verify our model and to identify sources of the mode two seed light. However, our model for thermal mode coupling appears to agree at least qualitatively with certain reported behaviors of laboratory amplifiers: a sharp pump threshold for mode degradation is predicted and reported; the pump power threshold is in the observed range; the frequency offset of 2-3 kHz for maximum gain agrees with reported fluctuation times; the mode coupling gain occurs primarily in the first half of the amplifier which is consistent with observations that coiling the first half of the amplifier often suppresses mode degradation.

If our model can be more fully validated, it should prove useful in improving amplifier designs in order to raise the mode degradation threshold. For example, we can apply it to bent fiber and to fiber with non-step index profiles or non-step Yb doping profiles. It can be used to compare co-pumped and counter-pumped amplifiers and different pump spectra. We can systematically study trends with core to pump cladding size ratios, and the length variations this implies.

Acknowledgments

We thank Dr. C. Jauregui of Friedrich-Schiller-Univ., Jena and J. Edgecumbe of Nufern for illuminating discussions of modal instability in high power fiber amplifiers. Funding for this work was provided by the Defense Advanced Research Project Agency (DARPA) under grant #083081003 and Sandia National Laboratories through contract #1038955.